Acta Pharmaceutica Sinica B 2018;8(1):97–105

Chinese Pharmaceutical Association
Institute of Materia Medica, Chinese Academy of Medical Sciences

Acta Pharmaceutica Sinica B

www.elsevier.com/locate/apsb
www.sciencedirect.com

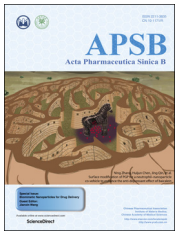

ORIGINAL ARTICLE

Biomimetic thiamine- and niacin-decorated liposomes for enhanced oral delivery of insulin

Haisheng He, Yi Lu, Jianping Qi, Weili Zhao, Xiaochun Dong, Wei Wu*

Key Laboratory of Smart Drug Delivery of MOE and PLA, School of Pharmacy, Fudan University, Shanghai 201203, China

Received 6 July 2017; received in revised form 14 September 2017; accepted 10 November 2017

KEY WORDS

Liposomes;
Vitamin;
Thiamine;
Niacin;
Insulin;
Biomimetic;
Oral;
Drug delivery

Abstract Biomimetic nanocarriers are emerging as efficient vehicles to facilitate dietary absorption of biomacromolecules. In this study, two vitamins, thiamine and niacin, are employed to decorate liposomes loaded with insulin, thus facilitating oral absorption *via* vitamin ligand–receptor interactions. Both vitamins are conjugated with stearamine, which works to anchor the ligands to the surface of liposomes. Liposomes prepared under optimum conditions have a mean particle size of 125–150 nm and an insulin entrapment efficiency of approximately 30%–36%. Encapsulation into liposomes helps to stabilize insulin due to improved resistance against enzymatic disruption, with 60% and 80% of the insulin left after 4 h when incubated in simulated gastric and intestinal fluids, respectively, whereas non-encapsulated insulin is broken down completely at 0.5 h. Preservation of insulin bioactivity against preparative stresses is validated by intra-peritoneal injection of insulin after release from various liposomes using the surfactant Triton X-100. In a diabetic rat model chemically induced by streptozotocin, both thiamine- and niacin-decorated liposomes showed a comparable and sustained mild hypoglycemic effect. The superiority of decorated liposomes over conventional liposomes highlights the contribution of vitamin ligands. It is concluded that decoration of liposomes with thiamine or niacin facilitates interactions with gastrointestinal vitamin receptors and thereby facilitates oral absorption of insulin-loaded liposomes.

© 2018 Chinese Pharmaceutical Association and Institute of Materia Medica, Chinese Academy of Medical Sciences. Production and hosting by Elsevier B.V. This is an open access article under the CC BY-NC-ND license (http://creativecommons.org/licenses/by-nc-nd/4.0/).

Abbreviations: AAC, area above the curve; CDI, *N*,*N*′-carbonyldiimidazole; CH, cholesterol; CH-Lip, conventional (cholesterol) liposomes; DMAP, dimethylaminopyridine; DMF, dimethylformamide; EDC, *N*-ethyl-*N*′-(3-dimethylaminopropyl) carbodiimide; EE, entrapment efficiency; ESI-MS, electrospray ionization mass spectrometry; FAE, follicle-associated epithelia; GIT, gastrointestinal tract; ^{1}H NMR, ^{1}H nuclear magnetic resonance; HPLC/UV, high-performance liquid chromatography/ultraviolet; INS, insulin; NA, niacin; NA-Lip, niacin liposomes; SGF, simulated gastric fluid; SIF, simulated intestinal fluid; SPC, soybean phosphatidylcholine; TH, thiamine; TH-Lip, thiamine-decorated liposomes; USP, United States Pharmacopeia; VB1, vitamin B1

*Corresponding author. Tel.: +86 21 51980084.
E-mail address: wuwei@shmu.edu.cn (Wei Wu).

Peer review under responsibility of Institute of Materia Medica, Chinese Academy of Medical Sciences and Chinese Pharmaceutical Association.

https://doi.org/10.1016/j.apsb.2017.11.007
2211-3835 © 2018 Chinese Pharmaceutical Association and Institute of Materia Medica, Chinese Academy of Medical Sciences. Production and hosting by Elsevier B.V. This is an open access article under the CC BY-NC-ND license (http://creativecommons.org/licenses/by-nc-nd/4.0/).

1. Introduction

The oral delivery of labile macromolecules such as polypeptides and proteins is one of the top challenges in the field of drug delivery[1–3]. The fact that only a few modestly successful oral macromolecular products are marketed indicates the difficulty of overcoming the various physiological barriers that impede the oral absorption of labile macromolecular entities[4]. There are two main challenges: issues of stability, either enzymatic or acidic, and trans-epithelial absorption[5,6]. After oral ingestion, labile biomacromolecules first encounter the harsh gastric and intestinal environment, and are broken down by either gastric acid or diverse enzymes throughout the gastrointestinal tract (GIT)[7–10]. Beyond the detrimental gastrointestinal environment, the epithelial lining guards the entrance to the circulatory system, allowing only small molecules with amicable properties such as a balanced hydrophilicity and hydrophobicity. To date, there are still no efficient strategies devised to tackle these two issues simultaneously. As a result, oral delivery of biomacromolecules remains a top research interest in both academics and industry, and workable approaches or vehicles are yet to be explored.

In recent years, nanovehicles have found wide application in the field of oral delivery[11–13]. Nonetheless, while nanovehicles are efficient in protecting the payloads, they create new problems as well; for example, enlarged particle size that renders oral absorption extremely difficult. However, the epithelial lining of the GIT is not entirely inaccessible to particles: Some pathogens such as bacteria and viruses have developed mechanisms of invasion into the circulatory system[14,15]. On the other hand, the GIT has evolved specific mechanisms to break down mass nutrients such as fats into small particles before absorption[16,17]. These examples suggest that we can break through these physiological barriers by mimicking biological processes.

By mimicking the invasion of pathogens, nanovehicles targeting M cells are able to be internalized and transported very quickly to follicle-associated epithelia (FAE) in the Peyer's patches[18–23]. Whatever the fate of the particles might be, trapped there or transported to other locations, new opportunities of oral delivery are created. However, due to the limited population of M cells, less than 1% of the total enterocyte population, attention has been drawn to targeting the enterocytes that are responsible for absorption of nutrients[24,25]. By targeting the receptors residing in the membranes of enterocytes, nanocarriers bearing payloads can be taken up *via* endocytosis, thus increasing the chance of delivering the nanovehicles to the circulatory system[26–28]. The decoration of the nanovehicles with ligands such as vitamins, amino acids and polypeptides endows them with biomimetic capabilities to work as Trojan horses to protect and transport the payloads into the body simultaneously[29–31]. Taking advantage of neonatal Fc receptors, insulin, encapsulated into poly(lactic acid-*co*-glycolic acid) (PLGA) nanoparticles, has been successfully delivered into the body and elicits therapeutic effects[32]. Vitamins such as folates, VB12 and biotins are among the most popular ligands for active targeting of the intestinal epithelia due to their versatility and availability[33–37]. In this study, we tested the feasibility of using two vitamins, thiamine (VB1) and niacin, as ligands for oral delivery. It has long been established that there is wide distribution of receptors for thiamine and niacin in the intestinal epithelia[38,39]. Therefore, it makes sense to decorate nanovehicles with thiamine and niacin for enhanced oral delivery. In this proof-of-concept study we employed liposomes as model vehicles and insulin as the model drug, both of which have been used extensively in our previous studies or by other researchers[36,40–47].

2. Materials and methods

2.1. Materials

Recombinant human insulin (INS) was provided by Jiangshu Wanbang Biopharmaceuticals Co., Ltd (Xuzhou, China). Cholesterol (CH) and soybean phosphatidylcholine (SPC, Lipoid S100) were supplied by Lipoid (Ludwigshafen, Germany). Sephadex G-50 was obtained from Pharmacia (Shanghai, China). Thiamine (TH) and niacin (NA) were purchased from Tokyo Chemical Industry Co., Ltd. (Tokyo, Japan). Stearamine was provided by Aladdin Industrial Corporation (Shanghai, China). *N*,*N*′-Carbonyldiimidazole (CDI), dimethylaminopyridine (DMAP), *N*-ethyl-*N*′-(3-dimethylaminopropyl) carbodiimide (EDC), phosphoric acid and triethylamine were supplied by Sinopharm Chemical Reagent Co., Ltd. (Shanghai, China). Streptozotocin was obtained from Sigma–Aldrich (Shanghai, China). Deionized water was prepared by a Milli-Q purification system (Millipore, Molsheim, France).

2.2. Synthesis of thiamine–stearamide and niacin–stearamide

TH–stearamide was synthesized utilizing CDI as a coupling reagent by the methods previously reported with modifications (Scheme 1)[48–50]. Briefly, 3 mmol TH and 3.6 mmol CDI were added to anhydrous dimethylformamide (DMF) to react for 24 h at room temperature. The activated TH (TH–CDI) was obtained by washing the reactants with cold anhydrous ether three times to remove DMF, residual CDI and other by products. Subsequently, 2.4 mmol TH–CDI and 2 mmol stearamine were allowed to react in anhydrous chloroform at 80 °C for 12 h. All reactions were conducted under the protection of nitrogen. After evaporation of chloroform, the product was purified by silica gel column using chloroform/methanol (20/1, *v*/*v*) and preparative high performance liquid chromatography with a mobile phase of acetonitrile/water successively.

NA–stearamide was synthesized by the common amidation reaction utilizing DMAP and EDC as catalysts by referring to our previous work[36]. Briefly, 1.0 mmol NA was dissolved in anhydrous dichloromethane, followed by addition of 1.5 mmol DMAP and 1.5 mmol EDC. After stirring for 30 min, 1.0 mmol stearamine was subsequently added and allowed to react at room temperature overnight under the protection of nitrogen under mild stirring. Upon evaporation of dichloromethane, water was added and extracted with ethyl acetate. After washing with 1 mol/L HCl, the organic phase was then dried with anhydrous sodium sulfate and concentrated in vacuum. The crude compound was finally purified by silica gel column using methanol/dichloromethane (1/20, *v*/*v*).

The chemical structures of TH–stearamide and NA–stearamide were confirmed by mass spectrometry (MS) and ^{1}H nuclear magnetic resonance (NMR), respectively.

2.3. Preparation of thiamine- and niacin-decorated liposomes

INS-loaded plain and decorated liposomes were prepared by a reversed-phase evaporation method following previous procedures with modifications[37,45]. The general procedures for preparation of

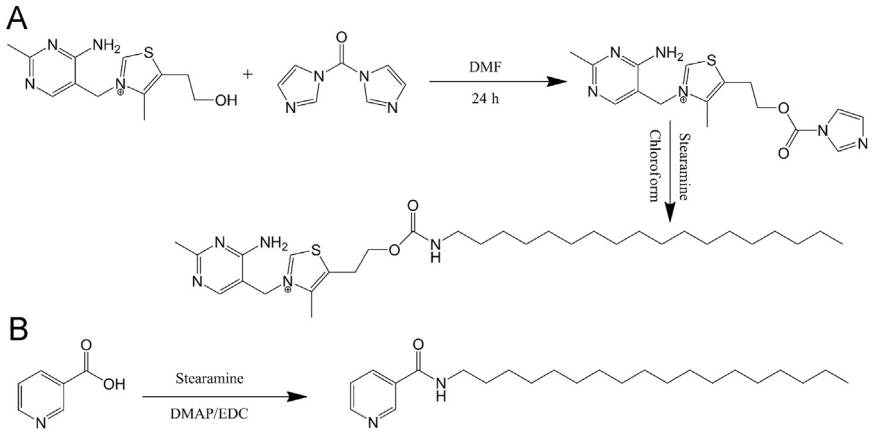

Scheme 1 Synthesis of TH–stearamide and NA–stearamide.

plain liposomes were as follows: dissolve SPC (225 mg, 0.3 mmol) and cholesterol (29 mg, 0.075 mmol) with 20 mL absolute ether; add 4 mL of INS hydrochloride solution (4 mg/mL); ultrasonicate for 1 min at 50% energy output to form the course emulsion; remove ether by a rotary evaporator at 37 °C; add 20 mL pH 5.4 citrate buffer pre-heated to 37 °C to hydrate for 2 h to get the crude liposomes; homogenize under high pressure to obtain INS-loaded liposomes.

Decorated liposomes were prepared following similar procedures. Nonetheless, since both TH–stearamide and NA–stearamide were sparely soluble in ether, they were first dissolved together with SPC and cholesterol using dichloromethane (NA–stearamide) or dichloromethane/methanol (TH–stearamide) and formed solid dispersions as thin films upon removal of the organic solvent. All downstream procedures were exactly the same as for preparation of plain liposomes. The total amount of 25.2 mg TH–stearamide (0.045 mmol) and 5.6 mg NA–stearamide (0.015 mmol) was added to the formulation to attain a coating density of about 15% and 5%, defined as conjugates/phospholipids in mole ratio, respectively.

2.4. *Characterization of liposomes*

Characterization of liposomes was performed following previous reported procedures[37,45]. The particle size was measured by dynamic light scattering using Zetasizer Nano ZS (Malvern, Worcestershire, UK). Gel permeation chromatography was employed to separate free INS from the liposomes using a 30 cm-long Sephadex G50 column, and entrapment efficiency (EE) was defined as the ratio of entrapped INS (INS_{ent}) to total INS (INS_{tot}) in Eq. (1):

$$EE\ (\%) = INS_{ent}/INS_{tot} \times 100\% \quad (1)$$

2.5. *Measurement of insulin using HPLC*

INS in formulations was measured by a reversed-phase HPLC/UV method as reported previously[45]. An Agilent 1200 series HPLC system (Santa Clara, USA) comprising of a quaternary pump, a degasser, an autosampler, a column heater and a tunable ultraviolet detector was employed to separate and detect INS. The chromatographic conditions were as follows: C18 column (Zorbax, 5 μm, 150 mm × 4.6 mm, Agilent, USA) with a C18 precolumn (20 mm × 2 mm); mobile phase: acetonitrile/0.57% phosphoric acid (adjusted to pH 2.25 with triethylamine) in a volume ratio of 26/74; column temp.: 25 °C; flow rate:1.0 mL/min; detection wavelength: 220 nm.

2.6. *Measurement of insulin bioactivity*

INS was first released from liposomes by disruption using 5% Triton X-100. The bioactivity was then evaluated in normal rats by measuring the hypoglycemic activity after intra-peritoneal injection at a dose of 2.0 IU/kg. For all experiments involving use of animals, guidelines issued by the ethical committee on animal welfare at School of Pharmacy, Fudan University were strictly followed. Blood samples were withdrawn from the tail vein before dosing and 0.25, 0.50, 1.0 and 2.0 h after dosing. Blood glucose levels were measured using glucose test strips (ACCU-CHEK, Roche). Bioactivity was expressed as percentages of post-dosing glucose levels relative to pre-dosing levels. Normal saline containing free INS was used as the positive control.

2.7. *In vitro stability of insulin*

The stability of liposomes was evaluated following previous procedures in both USP simulated gastric fluid (SGF, 0.32% pepsin, pH 1.2) and simulated intestinal fluid (SIF, 1% trypsin, pH 6.8)[44,46]. Briefly, 1 mL of INS-loaded liposome dispersion without removal of free INS was instilled into 4 mL of SGF or SIF thermostatically maintained at 37 °C and mechanically stirred at 100 rpm (SHZ-C, Shanghai Pudong Physico-Optical Instrument Factory, Shanghai, China). At time intervals, the samples were withdrawn and residual INS was analyzed by HPLC to evaluate the stability of the liposomes against acidic and enzymatic degradation.

2.8. *Hypoglycemic effect in rats*

Wistar rats weighing about 270 g were fasted for 24 h but allowed access to water before experiment. The diabetic rat model was induced by a single intra-peritoneal injection of streptozotocin at a dose of 60 mg/kg[51]. Three days after the initial injection, a second dose of streptozotocin, 20–60 mg/kg according to the actual blood glucose level, was given to rats with fasting blood glucose level lower than 16.7 mmol/L. Only when fasting blood glucose levels were over 16.7 mmol/L were the animals be used to evaluate the hypoglycemic effect of liposomes.

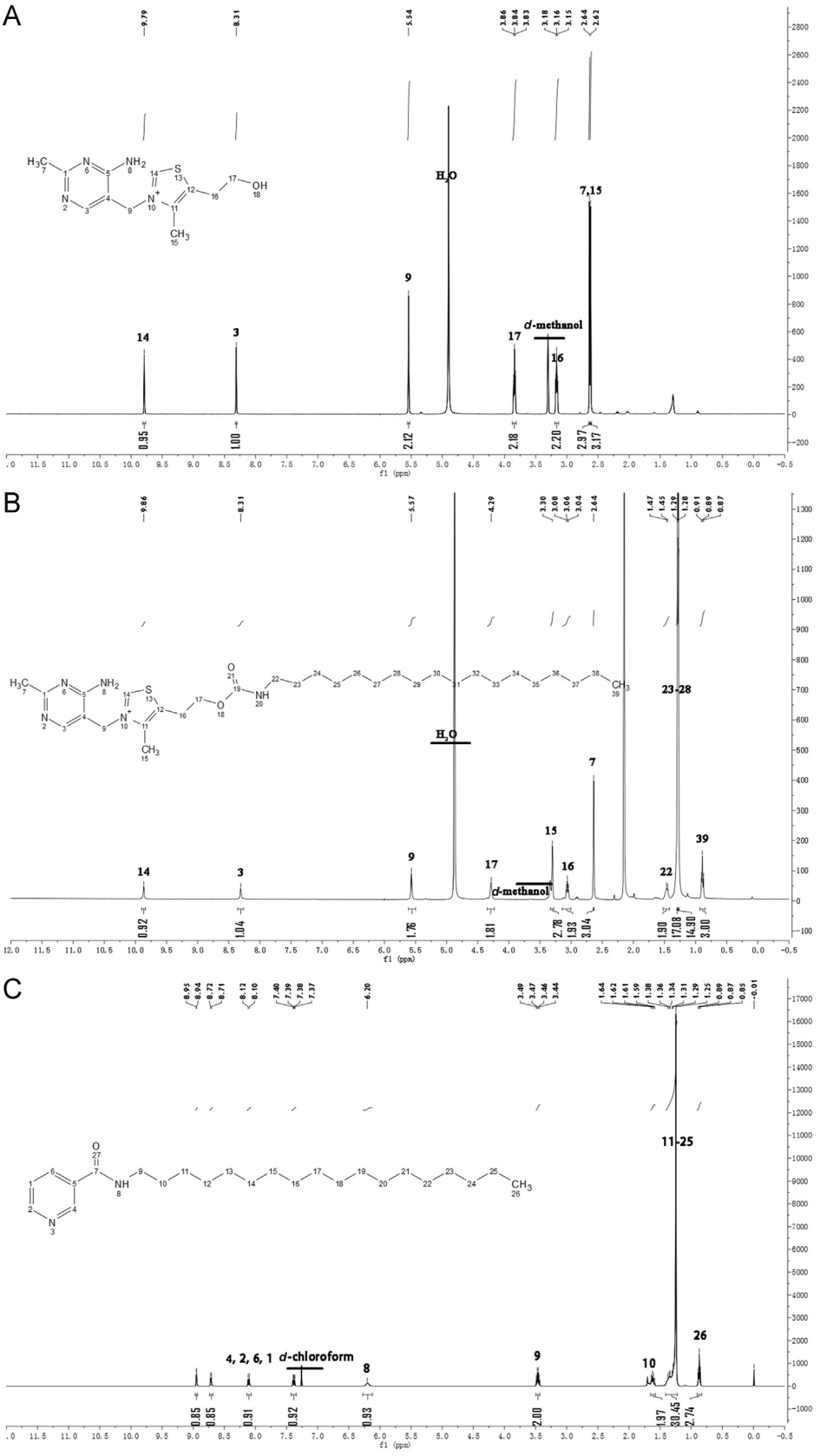

Figure 1 Mass spectra of TH (A), TH–stearamide (B) and NA–stearamide (C).

The diabetic rats were fasted overnight (12–14 h) but allowed free access to water. The rats were randomly divided into several groups, three in each group, and given various liposome formulations by gavage at a dose of 50 IU/kg with 2.0 IU/kg s.c. INS as a positive reference and normal saline as a sham control to mimic the stress upon administration. Blood samples were withdrawn from the tail vein and plasma glucose levels were measured using glucose test strips.

3. Results and discussion

3.1. Synthesis and identification of thiamine-stearamide and niacin-stearamide

Scheme 1 illustrates the synthetic scheme of TH–stearamide (Scheme 1A) and NA–stearamide (Scheme 1B), respectively. For the synthesis of TH–stearamide, CDI is utilized to activate the hydroxyl group of TH. Methanol has been reported to serve as the solvent for the activation due to excellent solubility of TH in methanol[48]. However, the abundant hydroxyl group of methanol may also react with CDI. To avoid the interference of methanol on the activation of TH by CDI, anhydrous DMF is used as the reaction medium to conduct a suspension reaction, which takes a relatively long time to complete[52]. The completion of reaction is judged by the disappearance of the peak at *m/z* of 265 in the MS spectrum, which corresponds to the $[M]^+$ of TH. TH–CDI is obtained and identified by MS with a sharp peak at *m/z* of 359, which is in accordance with the $[M]^+$ of TH–CDI. TH–stearamide is successfully synthesized by formation of the amino carbonate linkage between TH and stearamine. The structure of TH–stearamide is identified by MS and further confirmed by ^{1}H NMR (Fig. 1A and B). Electrospray ionization (ESI)-MS spectrum of TH–stearamide shows a major peak at *m/z* of 560, which belongs to the $[M]^+$ of TH–stearamide. Fig. 1A and B shows the ^{1}H NMR of TH and TH–stearamide, respectively. TH displays typical peaks of the protons in pyrimidine and thiazole segments at δ (ppm) = 8.3 and 9.8 (Fig. 1A), while TH–stearamide not only shows typical peaks of protons in TH at 9.9 and 8.3 ppm but also exhibits characteristic proton signals of CH_3– and –CH_2– in the alkyl chain of stearamine at 0.9, 1.3 and 1.5 ppm (Fig. 1B). Besides, the peak of neighbor protons of –CH_2– to hydroxyl groups in TH is shifted from 3.8 to 4.3 after conjugation of stearamine, further confirming the formation of the amino carbonate linkage.

NA–stearamide is successfully synthesized by the amidation reaction with DMAP and EDC as catalysts as well. After purification by silica gel column, a white powder (300 mg, 80%) is obtained. ESI-MS spectrum shows a major peak at *m/z* of 375, which corresponds to the $[M+H]^+$. As shown in Fig. 1C, NA–stearamide displays typical peaks of protons in pyridine at 7.4, 7.1, 8.7 and 9.0 ppm, as well as characteristic peaks of protons in the alkyl chain of stearamine at 0.9 and 1.3 ppm, confirming successful conjugation of NA with stearamine.

3.2. Preparation and characterization of insulin-loaded liposomes

Our previous study showed that INS-loaded liposomes with particle size of 150 nm displayed better hypoglycemic effect than

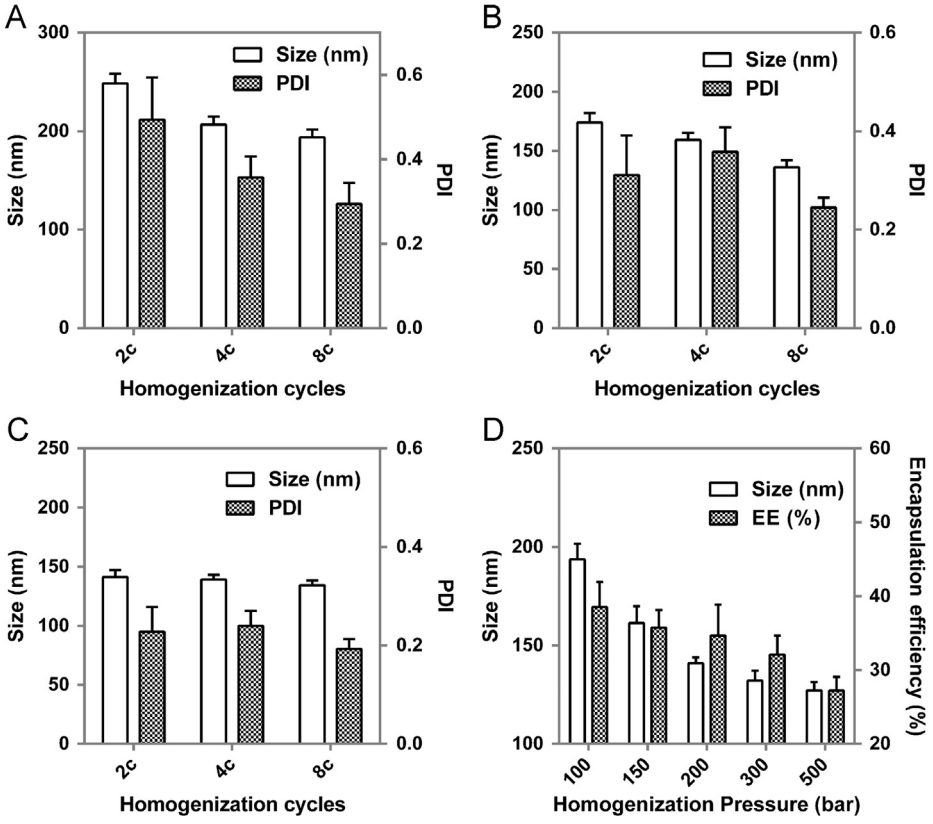

Figure 2 Effect of homogenization cycles on particle size and PDI of plain liposomes at 100 bar (A), 300 bar (B) and 500 bar (C); effect of homogenization pressure on particle size and entrapment efficiency (EE %) of liposomes (D).

Table 1 The particle size, PDI and entrapment efficiency of plain and decorated liposomes.

Formulation code	Decoration	Size (nm)	PDI	EE (%)
CH-Lip	/	148.0 ± 6.5	0.246	36.1 ± 3.1
NA-Lip	Niacin	135.7 ± 4.2	0.278	29.8 ± 1.9
TH-Lip	Thiamine	125.6 ± 2.9	0.224	30.6 ± 2.4

/, not applicable.

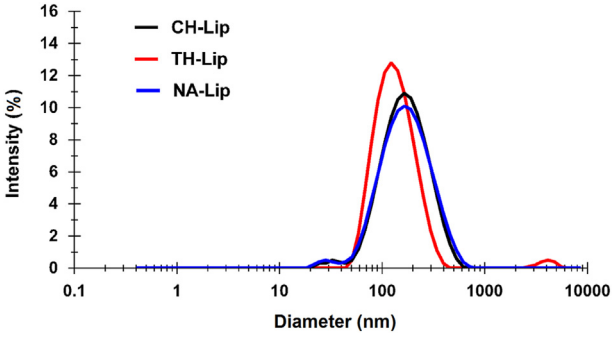

Figure 3 Particle size distribution of plain (CH-Lip) and TH- (TH-Lip) and NA-decorated (NA-Lip) liposomes prepared under optimized conditions.

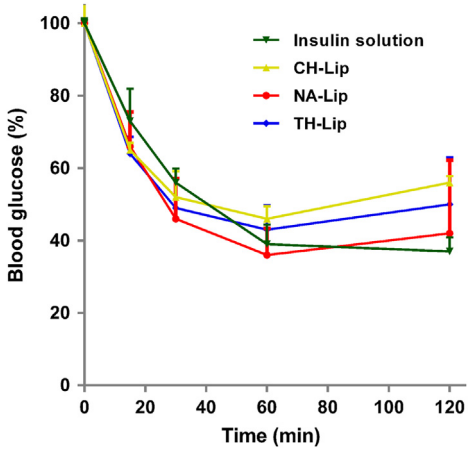

Figure 4 Profiles of bioactivity of INS-loaded liposomes, expressed as blood glucose levels at time points relative to the original levels before intra-peritoneal administration with INS solution as a reference ($n = 3$).

liposomes of other sizes[53]. Hence, this study aimed to prepare INS-loaded liposomes of 150 nm with good size distribution as well as high encapsulation efficiency of INS for further pharmacodynamic research. Fig. 2 shows the effect of homogenization parameters, including homogenization cycles and homogenization pressure on particle size, PDI and encapsulation efficiency. As shown in Fig. 2A–C, homogenization cycles have limited influence on particle size. With cycles increasing, particle sizes decrease slightly. Nevertheless, homogenization cycles have some impact on PDI, especially at low homogenization pressure, *e.g.* 100 bar. When cycles are over 8, PDI decreases to less than 0.3 at various pressures, which satisfies the requirements for a desired size distribution. With the homogenization cycles fixed at 8, the effects of homogenization pressure on particle size and encapsulation efficiency were investigated. Homogenization pressure was found to exert a significant influence on both particle size and encapsulation efficiency (Fig. 2D). Particle size showed a similar reduction trend with encapsulation efficiency when the pressure increased. However, the apparent reduction of particle size occurs at low pressure but at higher pressure for encapsulation efficiency. The liposomal particle size reaches 150 nm at a homogenization pressure of 150 and 200 bar. Nonetheless, 150 bar is preferred owing to the slightly higher encapsulation efficiency of INS.

Under optimized homogenization parameters, conventional INS-loaded liposomes (CH-Lip), NA- and TH-decorated INS-loaded liposomes (NA-Lip and TH-Lip) were prepared. The particle sizes, size distribution and encapsulation efficiency are shown in Table 1 and Fig. 3. In spite of the same preparation procedures, NA-Lip and TH-Lip were found to be slightly smaller than CH-Lip, which may be ascribed to the influence of NA–stearamide and TH–stearamide incorporated on the membrane fluidity of liposomes.

Our previous results showed that INS-loaded biotin-liposomes with a coating density of 20% produced the best hypoglycemic effect[53]. We tried to use similar coating density here. However, owing to the limited solubility of TH–stearamide in ether, the coating density of thiamine was tuned down to 15% to avoid possible precipitation during the preparative process. For niacin, the solubility in ether is even more limited, and 5% was the highest coating level that could be achieved. Above these levels, worries over precipitation of the coating agents increase substantially.

3.3. *Bioactivity of encapsulated insulin*

In the first half-hour blood glucose levels for liposomal groups drop more rapidly than in those administered free INS (Fig. 4). Although the underlying mechanisms need systematic investigation, it might be explained by the absorption-enhancing effect due to the presence of various surfactants that are present in the final formulation. At 2 h, the free INS solution is more efficacious than the three liposomal formulations in lowering blood glucose levels, and the liposomes differentiate as well. The observation at 2 h indicates relative bioactivity in the following order of free INS > NA-Lip > TH-Lip > CH-Lip. It is concluded that the bioactivity of encapsulated INS decreases slightly but the overall bioactivity is well preserved.

3.4. *Stability of insulin-loaded liposomes against acidic and enzymatic degradation*

In Fig. 5, it is obvious that free INS is degraded rapidly. At the first sampling time-point of 0.5 h, there is no INS left in the bulk solution (Fig. 5A). As for liposomal dispersions without separating the non-encapsulated fraction of free INS, residual INS drops to a level of about 20% in SGF (Fig. 5A) and 30% in SIF (Fig. 5C) of the original value at 0.5 h, at which it is maintained for an extended time duration. It is clear that this fraction of INS is

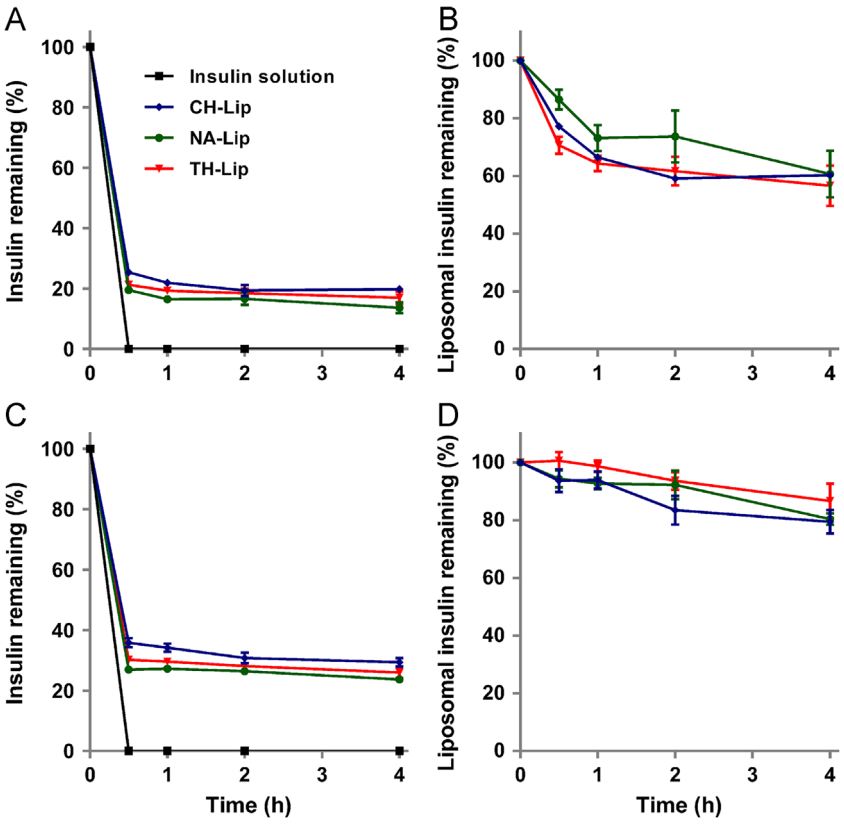

Figure 5 Stability of INS-loaded liposomes in SGF (A) and (B) and SIF (C) and (D) with INS solution as a control. Crude liposome dispersion without separating free INS is tested directly and the results are displayed as raw data (A) and (C) or calibrated data (B) and (D) by deducting the fraction of free INS in the liposome dispersions.

protected by the liposomes, whereas the fraction of degraded INS correlates to free INS in the dispersion. Since in Fig. 5A and C the protective effect of the liposomal vehicles has been concealed by the presence of a relatively large amount of free INS, the effect of the liposomal vehicles is highlighted by deducting the fraction of free INS from the total amount. Fig. 5B and D compare the protective effect of the three liposomes against destruction by SGF and SIF, respectively. At 4 h, about 40% and 20% of the encapsulated INS is degraded in SGF and SIF, respectively. Although the overall trend is comparable for the three liposomal formulations, surface coating with ligands seems to strengthen the liposomal vehicles against the damage caused by either acid or enzymes.

3.5. *Hypoglycemic effect of decorated liposomes in rats*

Upon chemical induction of diabetes with streptozotocin, the body weight of rats decreases dramatically from about 260 g to 240 g within 3 days, but the glucose levels of a majority of the animals fail to reach 16.7 mmol/L with a success rate of only 18.7% (Fig. 6). Nonetheless, after the second dose of streptozotocin, the blood glucose levels increase gradually and reach about 20 mmol/L after 2–3 weeks with a total success rate of 94% and a death rate of 6%.

After oral gavage with either TH- or NA-decorated liposomes, the hypoglycemic effect can be clearly observed (Fig. 7). The overall hypoglycemic effect of the two decorated liposome groups is comparable. In comparison with s.c. INS, the effect is mild and sustained for as long as 12 h. A rough estimation based on area above the curve (AAC) with the profile of the normal saline control as the baseline gives a relative oral bioavailability of about 2.5% for both TH- and NA-decorated liposomes. Although the calculated oral bioavailability is not as high as our previous results with biotin-decorated liposomes[36], the significantly enhanced bioavailability as compared with conventional liposomes, which show only a slight hypoglycemic effect, highlights the contribution of decoration with TH and NA as ligands.

It is found that NA-Lip achieve a greater hypoglycemic effect, with blood glucose levels as low as 72% of the original value; TH-Lips show a decrease of blood glucose levels to about 81%. If

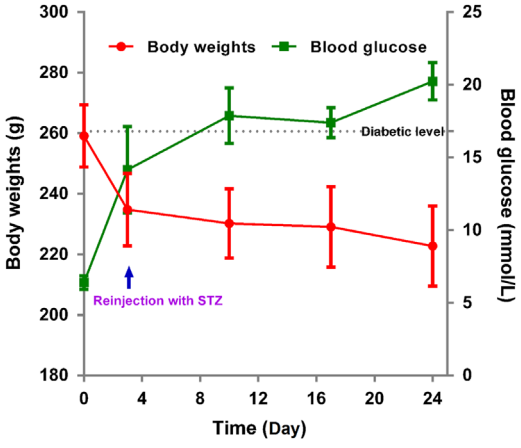

Figure 6 Profiles of body weight and blood glucose levels *vs.* time in response to chemical induction using streptozotocin.

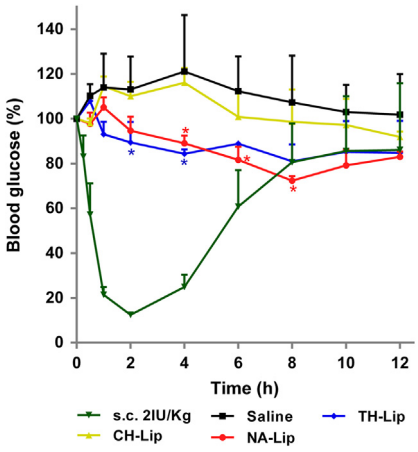

Figure 7 Blood glucose level after oral administration of INS-loaded liposomes at a dose of 50 IU/kg with INS solution as a control and s.c. INS at a dose of 2 IU/kg as a reference.

taking into account the 15% coating density of TH-Lip, the NA-Lip preparation with a coating density of just 5% seems to work better. Although the mechanisms are yet to be investigated, it is speculated that the amino–carbonate linkage in TH–stearamide might be unstable in the GIT and prone to degradation, which might compromise the efficacy of TH-decorated liposomes. However, NA–stearamide is linked through an amide bond and is more stable in the gastrointestinal environment. On the other hand, the GPR 109a receptor that is responsible for NA uptake have stronger bioactivity of endocytosis than the TH transporters such as Th Tr-1 and Th Tr-2[54–56]. Altogether, it is concluded that NA might outperform TH as a ligand to facilitate oral absorption of INS-loaded liposomes.

As observed from the profiles of blood glucose levels and compared with biotinylated liposomes in our previous study[36], the hypoglycemic effect of liposomes decorated with either vitamin is not as significant. The reasons might be ascribed to the limitations of the coating capacity of NA and the instability of the TH conjugate, as well as the possibility of less sensitivity of the diabetic rat model. The significantly higher degree of hypoglycemic effect of vitamin-decorated liposomes suffices to highlight the contribution of the ligands to overall oral absorption.

4. Conclusions

By conjugating with stearamine, both vitamins (TH and NA) were anchored onto the surfaces of liposomes *via* the lipid tag. Under optimum preparative conditions, all groups of liposomes have a mean particle size of 125–150 nm and an INS entrapment efficiency of 30%–36%. Encapsulation into liposomes stabilized INS against enzymatic catabolism in synthetic gastrointestinal secretions. INS bioactivity was well preserved against preparative stress. In a diabetic rat model induced by streptozotocin, both TH-Lip and NA-Lip showed a sustained, mild hypoglycemic effect. The superiority of decorated liposomes over conventional liposomes highlights the contribution of vitamin ligands. It is concluded that TH-Lip and NA-Lip mimic the absorption pathways of the corresponding vitamins and thereby facilitate the oral absorption of INS-loaded liposomes.

Acknowledgments

This work is financially supported by Shanghai Commission of Science and Technology (15ZR1403000), and National Natural Science Foundation of China (81573363, 81690263, and 21372063).

References

1. Luo YY, Xiong XY, Tian Y, Li ZL, Gong YC, Li YP. A review of biodegradable polymeric systems for oral insulin delivery. *Drug Deliv* 2016;**23**:1882–91.
2. Park JW, Kim SJ, Kwag DS, Kim S, Park J, Youn YS, et al. Multifunctional delivery systems for advanced oral uptake of peptide/protein drugs. *Curr Pharm Des* 2015;**21**:3097–110.
3. Shadab M, Haque S, Sheshala R, Meng LW, Meka VS, Ali J. Recent advances in non-invasive delivery of macromolecules using nanoparticulate carriers system. *Curr Pharm Des* 2017;**23**:440–53.
4. Hwang SR, Byun Y. Advances in oral macromolecular drug delivery. *Expert Opin Drug Deliv* 2014;**11**:1955–67.
5. Liu L, Yao W, Rao Y, Lu X, Gao J. pH-Responsive carriers for oral drug delivery: challenges and opportunities of current platforms. *Drug Deliv* 2017;**24**:569–81.
6. Niu Z, Conejos-Sánchez I, Griffin BT, O'Driscoll CM, Alonso MJ. Lipid-based nanocarriers for oral peptide delivery. *Adv Drug Deliv Rev* 2016;**106**:337–54.
7. Florence AT. Oral insulin delivery: a chimera?. *Int J Pharm* 2015;**495**:218–9.
8. Hetényi G, Griesser J, Moser M, Demarne F, Jannin V, Bernkop-Schnürch A. Comparison of the protective effect of self-emulsifying peptide drug delivery systems towards intestinal proteases and glutathione. *Int J Pharm* 2017;**523**:357–65.
9. Yadav V, Varum F, Bravo R, Furrer E, Basit AW. Gastrointestinal stability of therapeutic anti-TNFα IgG1 monoclonal antibodies. *Int J Pharm* 2016;**502**:181–7.
10. Leonaviciute G, Zupančič O, Prüfert F, Rohrer J, Bernkop-Schnürch A. Impact of lipases on the protective effect of SEDDS for incorporated peptide drugs towards intestinal peptidases. *Int J Pharm* 2016;**508**:102–8.
11. Abbad S, Zhang Z, Waddad AY, Munyendo WL, Lv H, et al. Chitosan-modified cationic amino acid nanoparticles as a novel oral delivery system for insulin. *J Biomed Nanotechnol* 2015;**11**:486–99.
12. Rekha MR, Sharma CP. Simultaneous Effect of thiolation and carboxylation of chitosan particles towards mucoadhesive oral insulin delivery applications: an *in vitro* and *in vivo* evaluation. *J Biomed Nanotechnol* 2015;**11**:165–76.
13. Horava SD, Moy KJ, Peppas NA. Biodegradable hydrophilic carriers for the oral delivery of hematological factor IX for hemophilia B treatment. *Int J Pharm* 2016;**514**:220–8.
14. Kochut A, Dersch P. Bacterial invasion factors: tools for crossing biological barriers and drug delivery?. *Eur J Pharm Biopharm* 2013;**84**:242–50.
15. Vela Ramirez JE, Sharpe LA, Peppas NA. Current state and challenges in developing oral vaccines. *Adv Drug Deliv Rev* 2017;**114**:116–31.
16. Mu H, Porsgaard T. The metabolism of structured triacylglycerols. *Prog Lipid Res* 2005;**44**:430–48.
17. Porter CJ, Trevaskis NL, Charman WN. Lipids and lipid-based formulations: optimizing the oral delivery of lipophilic drugs. *Nat Rev Drug Discov* 2007;**6**:231–48.
18. De Jesus M, Ostroff GR, Levitz SM, Bartling TR, Mantis NJ. A population of langerin-positive dendritic cells in murine Peyer's patches involved in sampling β-glucan microparticles. *PLoS One* 2014;**9**:e91002.
19. De Smet R, Demoor T, Verschuere S, Dullaers M, Ostroff GR, Leclercq G, et al. β-Glucan microparticles are good candidates for mucosal antigen delivery in oral vaccination. *J Control Release* 2013;**172**:671–8.

20. Xie Y, Jiang S, Xia F, Hu X, He H, Yin Z, et al. Glucan microparticles thickened with thermosensitive gels as potential carriers for oral delivery of insulin. *J Mater Chem B* 2016;**4**:4040–8.
21. Xie Y, Hu X, He H, Xia F, Ma Y, Qi J, et al. Tracking translocation of glucan microparticles targeting M cells: implications for oral drug delivery. *J Mater Chem B* 2016;**4**:2864–73.
22. Zhang X, Zhao Y, Xu Y, Pan Y, Chen F, Kumar A, et al. *In situ* self-assembly of peptides in glucan particles for macrophage-targeted oral delivery. *J Mater Chem B* 2014;**2**:5882–90.
23. Pooja D, Kulhari H, Kuncha M, Rachamalla SS, Adams DJ, Bansal V, et al. Improving efficacy, oral bioavailability, and delivery of paclitaxel using protein-grafted solid lipid nanoparticles. *Mol Pharm* 2016;**13**:3903–12.
24. Beloqui A, Brayden DJ, Artursson P, Préat V, des Rieux A. A human intestinal M-cell-like model for investigating particle, antigen and microorganism translocation. *Nat Protoc* 2017;**12**:1387–99.
25. Lopes MA, Abrahim BA, Cabral LM, Rodrigues CR, Seiça RM, de Baptista Veiga FJ, et al. Intestinal absorption of insulin nanoparticles: contribution of M cells. *Nanomedicine* 2014;**10**:1139–51.
26. Kaklotar D, Agrawal P, Abdulla A, Singh RP, Mehata AK, Singh S, et al. Transition from passive to active targeting of oral insulin nanomedicines: enhancement in bioavailability and glycemic control in diabetes. *Nanomedicine* 2016;**11**:1465–86.
27. Pawar VK, Meher JG, Singh Y, Chaurasia M, Surendar Reddy B, Chourasia MK. Targeting of gastrointestinal tract for amended delivery of protein/peptide therapeutics: strategies and industrial perspectives. *J Control Release* 2014;**196**:168–83.
28. Zhang X, Wu W. Ligand-mediated active targeting for enhanced oral absorption. *Drug Discov Today* 2014;**19**:898–904.
29. He R, Yin C. Trimethyl chitosan based conjugates for oral and intravenous delivery of paclitaxel. *Acta Biomater* 2017;**53**:355–66.
30. Xu Y, Xu J, Shan W, Liu M, Cui Y, Li L, et al. The transport mechanism of integrin $\alpha v\beta 3$ receptor targeting nanoparticles in Caco-2 cells. *Int J Pharm* 2016;**500**:42–53.
31. Zhang P, Xu Y, Zhu X, Huang Y. Goblet cell targeting nanoparticle containing drug-loaded micelle cores for oral delivery of insulin. *Int J Pharm* 2015;**496**:993–1005.
32. Pridgen EM, Alexis F, Kuo TT, Levy-Nissenbaum E, Karnik R, Blumberg RS, et al. Transepithelial transport of Fc-targeted nanoparticles by the neonatal fc receptor for oral delivery. *Sci Transl Med* 2013;**5**:213ra167.
33. Ke Z, Guo H, Zhu X, Jin Y, Huang Y. Efficient peroral delivery of insulin *via* vitamin B12 modified trimethyl chitosan nanoparticles. *J Pharm Pharm Sci* 2015;**18**:155–70.
34. Shen Y, Hu M, Qiu L. Sequentially dual-targeting vector with nano-in-micro structure for improved docetaxel oral delivery *in vivo*. *Nanomedicine* 2016;**11**:3071–86.
35. Roger E, Kalscheuer S, Kirtane A, Guru BR, Grill AE, et al. Folic acid functionalized nanoparticles for enhanced oral drug delivery. *Mol Pharm* 2012;**9**:2103–10.
36. Zhang X, Qi J, Lu Y, He W, Li X, Wu W. Biotinylated liposomes as potential carriers for the oral delivery of insulin. *Nanomedicine* 2014;**10**:167–76.
37. Verma AK, Sharma S, Gupta P, Singodia D, Kansal S, Sharma V, et al. Vitamin B12 grafted layer-by-layer liposomes bearing HBsAg facilitate oral immunization: effect of modulated biomechanical properties. *Mol Pharm* 2016;**13**:2531–42.
38. Rindi G, Laforenza U. Thiamine intestinal transport and related issues: recent aspects. *Proc Soc Exp Biol Med* 2000;**224**:246–55.
39. Said HM, Kumar C. Intestinal absorption of vitamins. *Curr Opin Gastroenterol* 1999;**15**:172–6.
40. Al-Remawi M, Elsayed A, Maghrabi I, Hamaidi M, Jaber N. Chitosan/lecithin liposomal nanovesicles as an oral insulin delivery system. *Pharm Dev Technol* 2017;**22**:390–8.
41. Manosroi A, Tangjai T, Sutthiwanjampa C, Manosroi W, Werner RG, Götz F, et al. Hypoglycemic activity and stability enhancement of human insulin–tat mixture loaded in elastic anionic niosomes. *Drug Deliv* 2016;**23**:3157–67.
42. Ohnishi N, Tanaka S, Tahara K, Takeuchi H. Characterization of insulin-loaded liposome using column-switching HPLC. *Int J Pharm* 2015;**479**:302–5.
43. Niu M, Tan Y, Guan P, Hovgaard L, Lu Y, Qi J, et al. Enhanced oral absorption of insulin-loaded liposomes containing bile salts: a mechanistic study. *Int J Pharm* 2014;**460**:119–30.
44. Hu S, Niu M, Hu F, Lu Y, Qi J, Yin Z, et al. Integrity and stability of oral liposomes containing bile salts studied in simulated and *ex vivo* gastrointestinal media. *Int J Pharm* 2013;**441**:693–700.
45. Niu M, Lu Y, Hovgaard L, Guan P, Tan Y, Lian R, et al. Hypoglycemic activity and oral bioavailability of insulin-loaded liposomes containing bile salts in rats: the effect of cholate type, particle size and administered dose. *Eur J Pharm Biopharm* 2012;**81**:265–72.
46. Niu M, Lu Y, Hovgaard L, Wu W. Liposomes containing glycocholate as potential oral insulin delivery systems: preparation, *in vitro* characterization, and improved protection against enzymatic degradation. *Int J Nanomed* 2011;**6**:1155–66.
47. Cui M, Wu W, Hovgaard L, Lu Y, Chen D, Qi J. Liposomes containing cholesterol analogues of botanical origin as drug delivery systems to enhance the oral absorption of insulin. *Int J Pharm* 2015;**489**:277–84.
48. Patel S, Gajbhiye V, Jain VK. Synthesis, characterization and brain targeting potential of paclitaxel loaded thiamine–PPI nanoconjugates. *J Drug Target* 2012;**20**:841–9.
49. Gajbhiye V, Jain NK. The treatment of glioblastoma xenografts by surfactant conjugated dendritic nanoconjugates. *Biomaterials* 2011;**32**:6213–25.
50. Zhang W, Shi Y, Chen Y, Ye J, Sha X, Fang X. Multifunctional Pluronic P123/F127 mixed polymeric micelles loaded with paclitaxel for the treatment of multidrug resistant tumors. *Biomaterials* 2011;**32**:2894–906.
51. Sharma G, Wilson K, Van der Walle CF, Sattar N, Petrie JR, Kumar MR. Microemulsions for oral delivery of insulin: design, development and evaluation in streptozotocin induced diabetic rats. *Eur J Pharm Biopharm* 2010;**76**:159–69.
52. Takamizawa A, Hamashima Y, Sato Y, Sato H, Tanaka S, Ito H, et al. Studies on pyrimidine derivatives and related compounds. XLI. 1 reaction of diethyl benzoylphosphonate with thiamine (Takamizawa Reaction 3). *J Org Chem* 1966;**31**:2951–6.
53. Zhang X, Qi J, Lu Y, Hu X, He W, Wu W. Enhanced hypoglycemic effect of biotin-modified liposomes loading insulin: effect of formulation variables, intracellular trafficking, and cytotoxicity. *Nanoscale Res Lett* 2014;**9**:185.
54. Thangaraju M, Cresci GA, Liu K, Ananth S, Gnanaprakasam JP, Browning DD, et al. GPR109A is a G-protein-coupled receptor for the bacterial fermentation product butyrate and functions as a tumor suppressor in colon. *Cancer Res* 2009;**69**:2826–32.
55. Hild W, Pollinger K, Caporale A, Cabrele C, Keller M, Pluym N, et al. G protein-coupled receptors function as logic gates for nanoparticle binding and cell uptake. *Proc Natl Acad Sci* 2010;**107**:10667–72.
56. des Rieux A, Pourcelle V, Cani PD, Marchand-Brynaert J, Préat V. Targeted nanoparticles with novel non-peptidic ligands for oral delivery. *Adv Drug Deliv Rev* 2013;**65**:833–44.